JGR Biogeosciences

RESEARCH ARTICLE
10.1029/2019JG005213

Sediment Properties Drive Spatial Variability of Potential Methane Production and Oxidation in Small Streams

P. Bodmer[1], J. Wilkinson[1], and A. Lorke[1]

[1]Institute for Environmental Sciences, University of Koblenz-Landau, Landau, Germany

Abstract Emissions of the potent greenhouse gas methane (CH_4) from streams and rivers are a significant component of global freshwater methane emissions. The distribution of CH_4 production and oxidation within stream sections and in vertical sediment profiles is not well understood, and the environmental controls on CH_4 production and emission in such systems create a significant challenge for assessing larger-scale dynamics. Here we investigate factors driving the spatial variability of sediment potential methane production (PMP) and potential methane oxidation (PMO) in a temperate stream network in Germany. PMP was highly variable, ranging from 5×10^{-4} to 28.58 μg CH_4 gDW^{-1} d^{-1} and PMO ranged from 0.43 μg CH_4 gDW^{-1} d^{-1} to 14.41 μg CH_4 gDW^{-1} d^{-1}. Important drivers of spatial variability of PMP and PMO in the sediments of the stream main-stem were related to fine sediment fraction and organic carbon content. At smaller spatial scale, that is, in a sub-catchment stream section, the drivers were more complex and included sediment nitrogen and organic carbon content, as well as porewater dissolved organic carbon, dissolved organic matter quality, and metal concentrations. As with reservoirs and impounded rivers, fine sediment deposition and organic carbon content were found to be key controls on the spatial variability of CH_4 production and oxidation. These findings enhance our understanding of CH_4 dynamics, improve the potential for identifying CH_4 production hotspots in small streams, and provide a potential means for upscaling emission rates in larger-scale assessments.

Plain Language Summary Globally, streams and rivers emit a significant amount of the highly potent greenhouse gas methane. The methane emitted from streams is mainly produced in sediments. The distribution of production and consumption in stream sections and sediment profiles is not well understood, which creates a significant challenge for estimating, for example, regional methane emissions from streams and rivers. We investigated possible factors controlling the variability from site to site and different depths of methane production and consumption in sediments of a stream network in south-west Germany. Sediment properties, the amount of fine sediment and organic carbon content, were key drivers of this variability in the main stream. In a smaller side arm of the main stream, the drivers were more complex, including nitrogen and organic carbon content of the sediment, but also porewater dissolved organic carbon, dissolved organic matter quality, and metals. As for reservoirs and dammed rivers, the accumulation of fine sediments and organic carbon content was found to be key controls of sediment methane production and consumption. These findings enhance our understanding of methane dynamics, improve the potential for identifying methane production hotspots in small streams, and provide a potential means for upscaling emission rates in larger-scale assessments.

Key Points:
- Sediment potential methane production (PMP) and oxidation (PMO) varied over five and two orders of magnitude, respectively in a temperate stream
- Main drivers of spatial variability of sediment PMP and PMO in the stream main-stem were mostly related to sediment properties
- Fine sediment deposition is a key control of sediment methane production in small streams

Supporting Information:
- Supporting Information S1

Correspondence to:
P. Bodmer,
bodmerpascal@gmail.com

Citation:
Bodmer, P., Wilkinson, J., & Lorke, A. (2020). Sediment properties drive spatial variability of potential methane production and oxidation in small streams. *Journal of Geophysical Research: Biogeosciences*, *125*, e2019JG005213. https://doi.org/10.1029/2019JG005213

Received 20 APR 2019
Accepted 21 DEC 2019
Accepted article online 5 JAN 2020

The copyright line for this article was changed on 23 APRIL 2020 after original online publication.

Author Contributions:
Conceptualization: P. Bodmer, A. Lorke
Data curation: J. Wilkinson
Formal analysis: P. Bodmer, J. Wilkinson
Funding acquisition: A. Lorke
Investigation: P. Bodmer
Methodology: P. Bodmer, J. Wilkinson
Project administration: P. Bodmer
Resources: A. Lorke
Supervision: A. Lorke
(continued)

1. Introduction

Natural sources, including freshwaters, account for about 35–50% of the global CH_4 emissions (Ciais et al., 2013). Freshwater CH_4 emissions are sensitive to climate change and expected to increase in the future (Campeau & Del Giorgio, 2014; Hamdan & Wickland, 2016). Moreover, estimates of freshwater CH_4 emissions from lentic and lotic systems represent an important source of uncertainty in the global CH_4 budget due to high spatial and temporal variability of fluxes and very uncertain surface areas (Saunois et al., 2016).

Measurements of CH_4 emissions from lotic freshwaters are less common compared to those from wetlands and lakes (but see e.g., Kling et al., 1992; Reeburgh et al., 1998; Crawford et al., 2013; Crawford et al., 2014). However, a recent review of Stanley et al. (2016) demonstrated the potential importance of streams and rivers in the global CH_4 budget, suggesting annual global stream emissions are equivalent to 15% of wetland and 40% of lake emissions.

Validation: P. Bodmer, J. Wilkinson
Visualization: P. Bodmer
Writing - original draft: P. Bodmer
Writing – review & editing: P. Bodmer, J. Wilkinson, A. Lorke

Methanogenesis in freshwaters mainly occurs in the sediment, where anoxic conditions prevail (Bastviken, 2009). Besides production by methanogenesis, CH_4 in freshwater systems is subject to microbial aerobic or anaerobic methane oxidation, although the latter appears less important in freshwaters (Bastviken, 2009; Cadieux et al., 2016; Oswald et al., 2015). Sawakuchi et al. (2016), for example, found that methane oxidation reduced the diffusive CH_4 flux by approximately 28–96% in the Amazon River mainstream and in its five largest tributaries. Hence, microbial CH_4 oxidation can be an important process moderating CH_4 emissions from aquatic systems.

Controls of CH_4 production in running waters can be categorized as proximal and distal (Stanley et al., 2016). Proximal controls on in situ methanogenesis, include sediment quantity, temperature, organic matter composition, macro-nutrients (nitrogen and phosphorus), and alternative electron acceptors. Sediment composition and properties seem to play an important role in CH_4 production in streams (Comer-Warner et al., 2018; Romeijn et al., 2019). Distal controls such as land utilization, hydrology, and geomorphology determine the supply of fine, organic-rich material and its spatial deposition patterns (see detailed discussion in Stanley et al., 2016). The combination of these multiple controls on CH_4 production, oxidation, and evasion rates all contribute to the poorly understood spatial and temporal variability of CH_4 concentrations and fluxes in lotic systems (Stanley et al., 2016).

The spatial variability of biogeochemical transformation rates is known to depend on spatial scale (Bernhardt et al., 2017; Palmer et al., 1997), that is, the larger the scale investigated, the greater will be the variability within that area. This may be complicated when comparing channels with different riparian land use and connectivity or with different levels of channel modification by transverse structures. Local changes in hydraulic geometry with lower flow velocity and enhanced sediment deposition have been found to coincide with hot spots of CH_4 emissions from impounded rivers (Maeck et al., 2013).

Methane production in sediments has been quantified by measuring rates of potential methane production (from here on referred as PMP) under optimal (i.e., anaerobic) conditions in laboratory incubations (Wilkinson et al., 2015; Bednařík et al., 2017; Crawford et al., 2017; Wilkinson, Bodmer, et al., 2019). In contrast to atmospheric emission rates, which exhibit strong temporal variation at timescales of minutes to days (Campeau & Del Giorgio, 2014; McGinnis et al., 2016), sediment PMP (controlled by slowly-varying sediment temperature) has been demonstrated to be equivalent to highly dynamic methane ebullition from river impoundments over annual cycles (Wilkinson et al., 2015; Wilkinson et al., 2019). The latter studies found a consistent decrease in PMP with increasing sediment depth, suggesting that the uppermost ca. 20 cm dominates CH_4 production in such sediments. It is unclear if such relationships exist in small streams, where the hydrodynamic conditions controlling sediment transport and accumulation are very different to those in river impoundments. In small streams, the rate of potential aerobic methane oxidation (from here on referred as PMO) may play a more important role in the sediment methane budget than in the strictly anaerobic sediments of river impoundments (e.g., Bednařík et al., 2017; Shelley et al., 2014; Shelley et al., 2017). The investigation of drivers of PMP and PMO spatial variability at specific depth layers is facilitated by laboratory sediment incubations, which additionally standardize their strong temperature-dependence (Aben et al., 2017; Yvon-Durocher et al., 2014).

To broaden the understanding of CH_4 emissions from stream and river networks, PMP and PMO, and their causal sediment and porewater characteristics in a small stream system (Strahler stream order 2–4), were investigated. To investigate spatial variability, sampling was evenly distributed along a 70-km stream main-stem, as well as a smaller (ca. 5 km) sub-catchment stream section to test whether controls on PMP and PMO differed from those at the larger scale. The findings are discussed in relation to potential up-scaling of CH_4 dynamics in fluvial networks in the context of global change.

2. Materials and Methods

2.1. Study Site

Sediments were collected from two reaches of the 271-km^2 Queich river catchment in Rhineland-Palatinate State, Germany (Figure 1). The streams are classified as fine-substrate dominated, siliceous highland streams (Dahm et al., 2014). The relatively pristine headwaters are located in the Palatinate forest (49°10′06″N 7°50′48.4″E), while the lower reaches pass through the intensively cultivated upper Rhine valley and enter

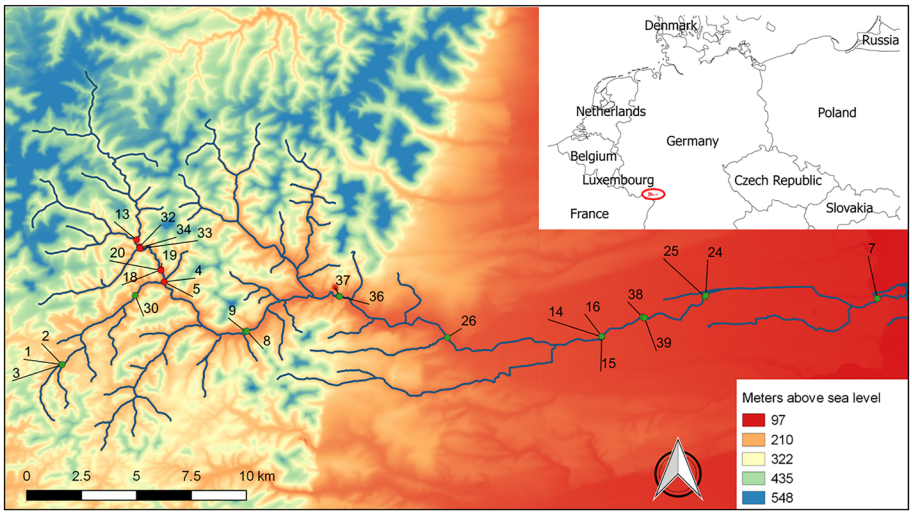

Figure 1. The study site with catchment location (inset top right) and sediment sampling sites in the main-stem (green spots) and sub-catchment stream (red spots) with core ID numbers (inset background: TM_WORLD_BORDERS-0.3; main map: 25-m digital elevation map, ©GeoBasis-DE/LVermGeoRP(2017)).

the Rhine River at 49°13′39″N 8°23′4″E. The main-stem was sampled at regular intervals over a 70-km stretch (spanning Strahler stream orders 2–4; Figure 1; hereafter referred to as main-stem). The second reach spanned ca. 5 km of the Wellbach stream sub-catchment (catchment area: 59 km^2, Strahler stream order 3; hereafter referred to as sub-catchment stream). Water depth ranged from 30 to 60 cm and stream wetted width from 2 to 9 m in the main-stem sampling sites, and water depth ranged from 20 to 50 cm and stream wetted width from 3 to 6 m in the sub-catchment stream.

2.2. Sampling Design

By spacing the sampling sites along the study stream from the headwaters to the lower part of the river, we aimed to capture all sediment types ranging from fine-grained sediment to coarse gravel. Ease of access was a contributing factor in sample site choice and, consequently, distance intervals. Multiple cores were taken from 13 sites between 2 and 22 August 2016. To minimize systematic sampling bias, one site in the sub-catchment stream and various sites in the main-stem were sampled on each sampling day. To minimize disturbance of the depth profile, coring tubes (inner diameter 59 mm; plexiglas) were pushed into the sediment by hand. In total, 17 cores from the main-stem and 9 from the sub-catchment stream were taken, with average core length (± standard deviation [SD]), 23 (± 8) cm (Bodmer et al., 2019). Cores were stored at 4–6 °C and processed in our laboratory within 1 week. At each site, we measured stream water temperature with a portable multimeter (3430 IDS, WTW GmbH, Germany). A further 1 L of stream water was collected at each site, for use in determination of PMO in surface water and in sediments (see below).

2.3. Porewater Extraction, Sediment Processing, and Calculations of PMP and PMO

Sediment porewater was extracted in the laboratory from 1-, 3-, 5-, and 10-cm depth below the sediment-water interface (SWI). Where pronounced changes in sediment structure were observed below 10-cm depth, these specific layers were also sampled ($n = 4$). Overlaying water was siphoned off to within a few centimeters of the SWI, and 13 ± 3.6 ml (average ± SD of all samples) of porewater was sampled. Extraction was performed from core side-wall holes using rhizon tubes (pore size: 0.15 μm; Rhizosphere Research Products B.V., Netherlands) connected by canule and septum sealed (nitrogen-flushed and evacuated) vials (21-ml volume) (Shotbolt, 2010). This porewater extraction approach can result in cross sampling from layers beyond the intended sampling depth. However, distinct differences in the characteristics of neighboring porewater samples suggest that cross sampling was minimal (for further information see supporting information, Figure S1). Filled vials were equilibrated to atmospheric pressure using a nitrogen-filled gas-bag connected by canule and septum, prior to vigorous shaking for 2 min to equilibrate porewater and headspace gases. The partial pressure of CH_4 and CO_2 in the vials was measured in a closed loop with an

Ultraportable Greenhouse Gas Analyzer (UGGA, model 915-0011, Los Gatos Research Inc., Mountain View Calif., USA) according to Wilkinson, Bors, et al. (2018, 2019). The equilibration temperature (i.e., water temperature) was measured in the first and last vial of the sample batch, and the final dissolved concentration was calculated according to Bossard et al. (1981) while using the solubility equation for CH_4 and CO_2 provided by Goldenfum (2010).

Sediment cores were processed in a nitrogen-flushed glove box, that is, with low oxygen environment, ca. 4% of atmospheric oxygen content. Cores were installed vertically through a clamped and O-ring-sealed port in the base of the box. Sediment was pushed upward within the core tube and sampled at layers coinciding with porewater extraction depths as described above. At each depth, a 5-ml sub-sample was taken with cut-off syringe and weighed, prior to wet bulk density determination according to Sekellick et al. (2013).

Sediment was sliced at ± 1 cm (for the first cm ± 0.5 cm) around each desired depth, homogenized, and subsamples were transferred into two pre-weighed nitrogen-flushed incubation vials. Smaller 20-ml vials were used for sandy sediments (expecting low PMP) and 125-ml vials for finer sediments (anticipating higher PMP). Large woody debris, leaves, and invertebrates were removed to minimize their potential to bias PMP away from that of the general sediment mass. Between 2.7 and 16.3 g of wet sediment (less for high producing silty sediment and more for sandy sediment) were transferred into each incubation vial. The duplicate vials were crimp-sealed with butyl rubber stoppers, weighed, and stored in darkness at 16 °C. This approached the in situ stream water temperature (average 14.5 °C) at sampling. PMP vial headspace gas methane and CO_2 was determined weekly, for 4 weeks, by withdrawing 100 µl samples using a gas-tight syringe (1710RN, 100 µl, Hamilton, Switzerland). Analysis followed the procedure for porewater gases described above (Wilkinson et al., 2018; Wilkinson et al., 2019). PMP for all cores, depths, and duplicate vials was calculated from the linear increase in headspace CH_4 partial pressure over time as described in Wilkinson et al. (2015; supporting information, Figure S2). PMP experiments proceed under anaerobic conditions; although some methane consumption in the test vials by anaerobic methane oxidization is possible, it was not quantified.

PMO was estimated for duplicate sediment subsamples from 1, 3, and 5 cm below the SWI, respectively. We transferred 0.2–1.7 g of wet sediment depending on expected PMO intensity (as for PMP, less silty sediment and more sandy sediment) into pre-weighed 10-ml incubation vials and added ca. 5-ml oxygenated stream water from the corresponding sampling location. The vials were sealed as for PMP. Vial headspaces were enriched by adding 10-µl pure methane gas (Methane 4.5, purity 99.998 %, Messer Schweiz AG, Switzerland), using a gas-tight glass syringe (1710RN, 100 µl, Hamilton, Switzerland), and giving an initial concentration of 2,317 nmol l^{-1} ± 14% SD in the sediment-water slurry (Shelley et al., 2014). Although PMO is concentration dependent (Shelley et al., 2015), to compare the capacity for methane oxidation in different sediments, we used a standardized initial injection rather than the measured porewater concentration. There was no significant correlation between initial methane concentration and PMO ($R^2 = -0.01$, $p = 0.89$; supporting information, Figure S3), and since the main aim of this study was to find links to environmental parameters, this uncertainty was considered acceptable. The prepared vials were re-weighed, and the 5-day PMO incubation experiment was carried-out on a shaker, at 16 °C in darkness. The first measurement of headspace CH_4 partial pressure was made after 30 min of shaking, as described for PMP, and the vials were measured daily. The rate of PMO was calculated from the linear decrease in total CH_4 content (headspace and sediment-water slurry; Shelley et al., 2014) over the first 3 days of measurement combining both respective replicates (supporting information, Figure S4). Surface water PMO at each site was determined in triplicates following the procedure described above.

On completion of PMP and PMO measurements, the sediment from each incubation vial was oven dried at 100 °C for ca. 30 hr, and calculated PMP and PMO rates were normalized to the respective sediment sample dry weight (DW; i.e., µg CH_4 gDW^{-1} d^{-1}).

2.4. Porewater Characterization

Sediment porewater samples were processed on the day of extraction. A 1-ml aliquot, diluted 10 times with MilliQ, preserved with 100-µl HNO_3, was stored at 4 °C prior to analysis of cation and metal concentrations (Na, Mg, K, Mn, Fe, Cu, and Zn expressed in µg l^{-1}) by inductively coupled plasma optical emission spectrometry (ICP-OES 720, Agilent, United States, column: 6.1006.630 Metrosep A Supp 7 – 250).

Table 1
Variables Used for Partial Least Square (PLS) Analysis in the Main-Stem and Sub-Catchment Stream (Indicated as Yes or No)

Variable	Description (unit)	Main-stem	Sub-catchment stream
Y variables in PLS			
PMP	Potential methane production rate (μg CH_4 gDW^{-1} d^{-1})	Yes[b]	Yes[b]
PMO	Potential methane oxidation rate (μg CH_4 gDW^{-1} d^{-1})	Yes[b]	Yes[b]
Sediment *X* variables in PLS			
D	Depth below sediment-water interface (cm)	Yes[b]	Yes[b]
ρ_{wb}	Wet bulk density (g cm^{-3})	Yes	Yes[b]
GS_clay	Grain size class clay, <2 μm (vol%)	Yes[a]	Yes[a]
GS_silt	Grain size class silt, 2–63 μm (vol%)	Yes[a]	Yes[a]
GS_sand	Grain size class sand, 63–2,000 μm (vol%)	Yes	Yes
GS_gravel	Grain size class >2,000 μm	Yes[a]	Yes[a]
C_{org}	Organic carbon content (mass%)	Yes[a]	Yes[a]
N	Nitrogen content (mass%)	No	Yes
Porewater *X* variables in PLS			
CH4_conc	CH_4 concentration (μM)	Yes[b]	Yes[b]
CO2_conc	CO_2 concentration (μM)	Yes[b]	Yes[b]
DOC	Dissolved organic carbon (mg l^{-1})	Yes[b]	Yes[b]
Cl	Chloride (mg l^{-1})	No	Yes[b]
SO4	Sulfate (mg l^{-1})	Yes[b]	Yes[b]
K	Potassium (μg l^{-1})	Yes[b]	Yes
Mg	Magnesium (μg l^{-1})	Yes[b]	Yes[b]
Mn	Manganese (μg l^{-1})	Yes[b]	Yes[b]
Na	Sodium (μg l^{-1})	Yes[b]	Yes
Zn	Zinc (μg l^{-1})	Yes[b]	Yes
Fe	Iron (μg l^{-1})	Yes[b]	Yes[b]
SUVA254	Specific UV absorption at 254 nm	Yes[b]	Yes[b]
E4:E6	E4:E6, a proxy for DOM aromaticity	Yes[b]	Yes[b]
a440	a440, a proxy for the amount of humic substances in DOM	Yes[b]	Yes[b]
a254:a365	a254:a365, proxy for DOM molecular weight	Yes	Yes
Sr	Slope ratio, a proxy for DOM molecular weight	Yes[b]	Yes[b]
E2:E3	E2:E3, a proxy for molecule size	Yes	Yes
HIX	Humification index, a proxy for the extent of humification	Yes	Yes
FI	Fluorescence index, a proxy for DOM source (i.e., terrestrial versus microbially derived DOM)	Yes	Yes
b:a	Freshness index, a proxy for fresh microbially produced DOM	Yes	Yes

Note. Category in PLS indicates dependent (Y) and independent (X) variables. The concentration of copper, fluoride, acetate, nitrite, nitrate, and phosphate in the porewater had to be excluded from both PLS analyses because of too few measurements above the detection limit.
Abbreviations: DOM = dissolved organic matter, PLS = partial least square, UV = ultraviolet.
[a]Data were arcsin-transformed prior to PLS analysis. [b]Data were log-transformed prior to PLS analysis.

A 3-ml aliquot was diluted three times and stored frozen prior to analysis for dissolved organic carbon (DOC in mg l^{-1}) using a multi N/C analyzer (2100S, Analytik Jena, Germany).

A further 8-ml aliquot was diluted two times and stored at 4 °C for absorbance and fluorescence measurements and analyzed within 5 days of extraction. These metrics provide proxies for the composition, intrinsic properties, source, or biological availability of dissolved organic matter (DOM; hereafter referred as DOM quality; see Table 1 for meaning of the calculated indices below; Jaffé et al., 2008; Fellman et al., 2010). Absorbance was measured at room temperature with a 1-cm cuvette at a ultraviolet (UV)/visible spectrophotometer (SPECORD 50, Analytik Jena, Germany) from 200 to 900 nm (1-nm increments). Samples with a higher absorption than 0.3 at 254 nm were additionally diluted (Kothawala et al., 2013). The data were corrected for blanks (MilliQ). Fluorescence was measured subsequently to absorbance measurements with a fluorescence spectrometer (LS 55, PerkinElmer, Inc., United States). We measured the excitation (244–380 nm, 0.5-nm steps) and the emission (290–510 nm, 5-nm steps) with a slit width of 5 nm for both excitation and emission to produce excitation-emission-matrices. The excitation-emission-matrices were corrected for

blanks (MilliQ) as well as for the inner filter effect with the absorbance based approach (Kothawala et al., 2013). A series of metrics were derived from the absorbance data: ratios E2:E3 and E4:E6 (Helms et al., 2008), absorption coefficient a440 (Cuthbert & Del Giorgio, 1992), specific UV absorption ($SUVA_{254}$) (Weishaar et al., 2003), absorption coefficients ratio a254:a365 (Dahlen et al., 1996; Dehaan, 1993), and the slope ratio (Sr; Helms et al., 2008). From fluorescence data, indices for freshness (b: a; Parlanti et al., 2000), fluorescence (FI; McKnight et al., 2001), and humification (HIX) (Ohno, 2002) were calculated (see Table 1).

Following absorbance and fluorescence analysis, residual samples were stored frozen awaiting anion analysis (for fluoride, acetate, chloride, nitrite, nitrate, phosphate, and sulfate concentration expressed in mg l^{-1}) by ion chromatography (881 Compact IC pro, Metrohm, Switzerland).

2.5. Sediment Characterization

Residual sediment, not used for PMP, PMO, or bulk density measurements, was frozen then freeze-dried. To characterize sediment organic carbon and nitrogen content (% DW), 15–20 mg of sediment was weighted into silver boats (11 × 4 × 4 mm), exposed to HCl (37%, 12 M) vapor for 6 hr to remove carbonates (Harris et al., 2001), and re-dried for 4 hr at 60 °C. Prior to analysis by dry combustion (Vario MICRO Cube, Elementar Analysensysteme GmbH, Germany), each silver boat was packed in larger tin boats with 20- to 30-mg tungsten trioxide (WO_3) to ensure complete combustion.

Grain size distribution was determined on a further portion of freeze-dried and pre-sieved (<2 mm) sediment, by laser-diffraction (particle size analyzer, CILAS 1190). Particles were maintained in suspension by stirring in deionized water. Aggregates were broken-down by ultrasonic agitation. Propanol was added to reduce water surface-tension and ensure mixing of floating organic matter. The analysis provided 20 grain size classes (0.04 and 2,500 μm, expressed as % volume), which were aggregated into four bulk classes: clay (<2 μm), silt (2–63 μm), sand (63–2,000 μm), and gravel sediment (>2,000 μm).

2.6. Comparison of PMP With Literature Data

Because methane production varies exponentially with temperature (Aben et al., 2017; Wilkinson et al., 2015; Wilkinson, Bodmer, & Lorke, 2019; Yvon-Durocher et al., 2014), direct comparison of quoted literature PMP values is often not possible due to the respective incubation temperatures used. For example, PMP from incubation at 10 °C cannot be compared to that incubated at 20 °C. Therefore, to compare our data with existing incubation studies, it was necessary to convert our PMP values to the temperatures. and units used in the literature (supporting information, Table S1). Wilkinson et al. (Wilkinson, Bodmer, & Lorke, 2019) demonstrated a consistent PMP thermal response coefficient θ, based on their own experiments and wide-ranging literature data. We applied this mean θ (0.041, SD ± 0.016), to convert our PMP rate to the temperature used in each other literature study, such that $PMP_{T\mathrm{lit}} = PMP_{T16}10^{\theta\Delta T}$, where $\Delta T = T_{\mathrm{lit}} - T_{16}$, T_{lit} is the target study incubation temperature, and T_{16} is 16 °C. PMP_{T16} and $PMP_{T\mathrm{lit}}$ are our PMP values incubated at 16 °C and PMP at T_{lit}, respectively.

2.7. Statistical Analysis

The analysis of drivers of PMP and PMO spatial variability for the main-stem and sub-catchment stream data was done separately in order to avoid a bias caused by the number of sampled sediment cores (17 from the main-stem and 9 from the sub-catchment stream).

Multivariate linear regression by means of partial least-squares (PLS) projections to latent structures (Eriksson et al., 2001; see Table 1) was used to identify the strongest predictors of PMP and PMO spatial variability (dependent Y variables) from measured environmental parameters (independent X variables). For PMP as well as PMO, all depths were included as single data points. PLS suits data sets with a large number of variables, can account for their collinearity, and deviation from normality, and is very tolerant of missing values (Sobek et al., 2007). Despite this, for the main-stem PLS analysis, porewater chloride concentration and sediment nitrogen content were excluded due to insufficient data above the detection limit. In order to improve model performance, highly skewed variables (skewness >2.0 and min/max ratio > 0.1) were either log- (continuous variables), or arcsin-transformed (discrete variables, i.e., grain size classes expressed as % volume). Data were scaled to unit variance and mean centered before running the PLS. The former was done to normalize the range of variables, while the latter reduces the influence of

multicollinearity (Iacobucci et al., 2016). Model validation was carried out using a permutation test. Y values were permutated 100 times and for each of the 100 new models, R^2Y and Q^2 were assessed. Moreover, X variables were grouped according to their relevance in explaining Y variables (variable importance in the projection [VIP]) according to Eriksson et al. (2001). VIP larger than 1.0 are highly influential, VIP between 1.0 and 0.8 are moderately influential, and VIP smaller than 0.8 are less influential. The results of the PLS are purely empirical and require careful interpretation for causal relationships. PLS and model validation were done in SIMCA 15.0.2 (Umetrics, Umeå, Sweden), for further information on these techniques see supporting information.

We performed linear regressions to investigate relationships between PMP and PMO. The reported R^2 values are adjusted for the number of data points. The significance of the regression slope was tested by analysis of variance (ANOVA) using a significance level (p) of 0.05.

3. Results

Median PMP rates in sediment cores from the main-stem and sub-catchment stream varied over five orders of magnitude, from 5×10^{-4} to 28.58 μg CH_4 gDW^{-1} d^{-1} (Figure 2a). Similar variability (5×10^{-4} to 15.27 μg CH_4 gDW^{-1} d^{-1}) was observed among cores from the main-stem (excluding sub-catchment stream data), while in the sub-catchment stream, median PMP values varied over four orders of magnitude from 4.5×10^{-3} to 28.58 μg CH_4 gDW^{-1} d^{-1}. PMO rates were less variable than PMP (Figure 2b). For PMO, median values for all sediment cores and for cores from the main-stem varied over two orders of magnitude, from 0.43 to 14.41 μg CH_4 gDW^{-1} d^{-1}. In the sub-catchment stream median, PMO rates per core varied over one order of magnitude, from 0.73 to 9.01 μg CH_4 gDW^{-1} d^{-1}. The surface water PMO was one to two orders of magnitude lower than the lowest PMO in the sediment.

Samples with high PMP tended to have high PMO ($R^2 = 0.43$, $p = 2 \times 10^{-10}$; Figure 3). Although PMO depends on CH_4 concentration, the relative magnitude of the measured PMO in μg CH_4 gDW^{-1} d^{-1} can nonetheless be compared to PMP. Our findings show that CH_4 production potential of the sediments exceeded their oxidation potential on average by 15%.

PMP and PMO variation at each sampled sediment depth was as great as that for all the data, varying over five and three orders of magnitude (supporting information, Figures S5a and S5b). Hence, there was no consistent pattern of vertical gradient in PMP, PMO, or any other measured variable (see examples in supporting information, Figures S6a–S6d).

The PLS model for spatial variability of PMP and PMO in the main-stem revealed two significant components that explained in total 72.1% of the variance ($R^2Y_{cum} = 0.721$; Figure 4a; Table 1). The model's predictive power was high ($Q^2_{cum} = 0.678$), while the background correlation assessed via model validation for PMP and PMO was low ($R^2Y = 0.138$ and 0.136, respectively). The loading plot (Figure 4a) shows that dependent (Y) variables, PMP and PMO, were strongly correlated to each other. The grain size class silt (GS_silt) was the most important predictor of PMP and PMO variability in the main-stem (Figures 5b and 5d). VIP values indicate other highly influential predictors of PMP and PMO variability. These include grain size class clay (GS_clay; Figures 5a and 5c) and sediment organic carbon content (C_{org}). In addition, porewater manganese concentration (Mn) was positively correlated (Figure 4a), whereas Mn had a distinctly lower VIP value compared to GS_silt, GS_clay, and C_{org}. Moreover, wet bulk density, (ρ_{wb}) as a highly influential predictor, was actually negatively correlated with PMP and PMO.

The loading plot derived from PLS also illustrates the correlation structure of the independent (X) variables. Sediment characteristics reflecting fine material and consequently high organic carbon content of sediment (GS_silt, GS_clay, and C_{org}) were strongly (positively) correlated as indicated by their position close to each other (Figure 4a). Characteristics for larger sediment grain size and density (GS_gravel and ρ_{wb}) and indices of porewater DOM—proxies of molecular weight or molecule size (a254:a365, E2:E3, Sr)—were (negatively) correlated. Moderately influential parameters for PMP and PMO included proxies of molecular weight and size of DOM (a254:a365, E2:E3, Sr), grain size larger 2 mm (GS_gravel), depth below SWI (D), porewater sulfate concentration (SO4; negatively correlated), proxies of humic substances and aromaticity (a440 and SUVA254), as well as porewater CH_4 concentration (CH4_conc, positively correlated). PMP and PMO

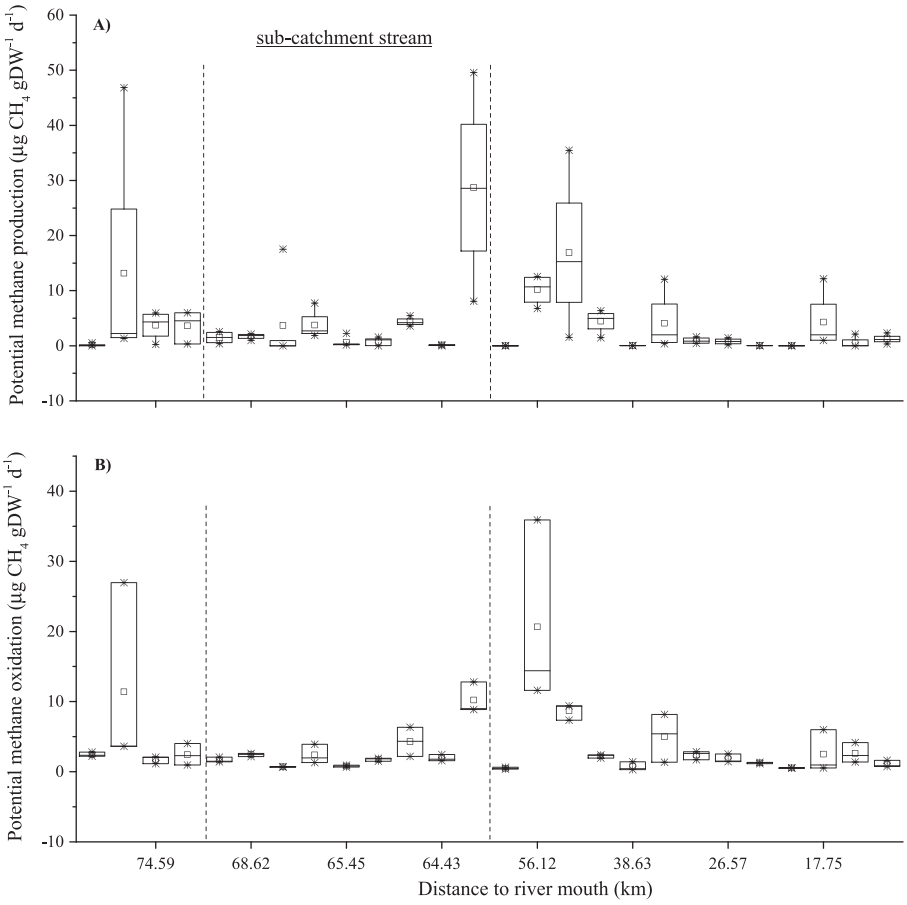

Figure 2. (a) Potential methane production (PMP) and (b) potential methane oxidation (PMO) ranges for each sediment core (incorporating data for all sub-sampled depths within each core). Box-Whisker plots show median (vertical line within box), average (open square), 25 and 75 percentiles (box), min/max value (vertical line outside box), the 1 and 99 percentile (cross), as well as the whisker (vertical line).

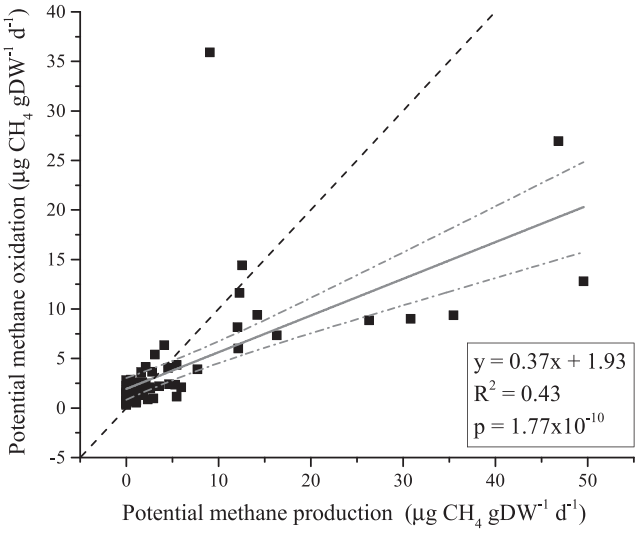

Figure 3. Relationship between potential methane production and potential methane oxidation. Grey line indicates linear regression provided in the legend; dash-dotted lines indicate 95% confidence interval; and dashed line indicates 1:1 line.

were little influenced by porewater DOC, Zn, K, Na, Fe, Mg, or dissolved CO_2 (CO2_conc), grain size class sand (GS_sand), proxies for freshness of DOM (b:a), humification (HIX), source of the DOM (FI), as well as another proxy for aromaticity (E4:E6).

The PLS analyzing the drivers of spatial variability of PMP and PMO in the sub-catchment stream resulted in a relatively high background correlation for both PMP ($R^2Y = 0.262$) and PMO ($R^2Y = 0.286$). This can be explained by the large number of independent variables (n = 28) compared to the number of observations (n = 39) as well as many missing data (i.e., measurements below the detection limit). However, the PLS analysis extracted two significant components which explained 70.4% of the variance ($R^2Y_{cum} = 0.704$) with a moderate predictive power ($Q^2_{cum} = 0.549$) relative to R^2Y (Figure 4b; Table 1). Compared to the main-stem, the dependent variables PMP and PMO had an even stronger correlation. Based on the VIP scores, organic carbon content (C_{org}) in the sediment was by far the most important predictor for spatial variability of PMP and PMO in the sub-catchment stream. Further highly influential predictors were sediment nitrogen content (N), porewater DOC, K, Na and Mg (positively correlated), as well as wet bulk density (ρ_{wb}), and the proxies

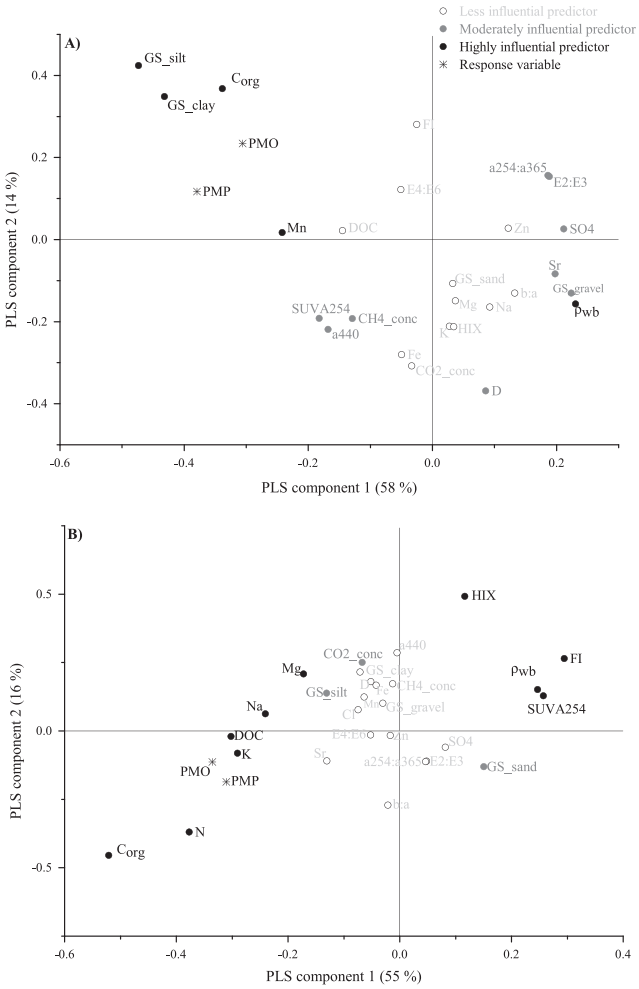

Figure 4. Partial least square (PLS) loading plot of potential methane production (PMP) and oxidation (PMO) in the main-stem (a) and in the sub-catchment stream (b) showing the correlation structure of dependent variables (asterisks) and independent variables (circles). Percentage values in axis labels are the proportion of PMP and PMO variability explained. Independent variables furthest from the plot origin (positive or negative) are the most influential predictors, and independent variables closest to the origin least influential. Independent variables close to the dependent variables are positively correlated; those on the opposite side of the origin are negatively correlated. See explanation of abbreviations in Table 1.

for humification (HIX), source (FI), and aromaticity (SUVA254) of DOM (negatively correlated). Moderately influential parameters are the grain size class silt (GS_silt) and CO_2 concentration (CO2_conc) in the porewater (positively correlated), as well as grain size fraction sand (GS_sand; negatively correlated). Less influential parameters for PMP and PMO in the sub-catchment stream were porewater CH_4 concentration (CH4_conc), the concentration of Fe, SO_4, Zn, Mn, and Cl in the porewater, the grain size classes clay and larger than 2 mm (GS_clay, GS_gravel), depth below SWI (D), as well as the proxies for the freshness (b:a), the molecular size (E2:E3), the molecular weight (a254:a365, Sr), and aromaticity (E4:E6) of the DOM in the porewater, as well as for humic substances in the DOM (a440).

4. Discussion

4.1. Drivers of Spatial Variability of PMP and PMO

The linear correlation (Figure 3), as well as close proximity in the PLS loading plot (Figure 4) of PMP and PMO, show a strong connection, indicating that both processes might be directly or indirectly controlled by similar drivers in the sediment, or dependent on each other. In the main-stem and sub-catchment stream, the key drivers of PMP and PMO spatial variability were related to sediment properties. For the main-stem, the strongest predictors of PMP and PMO were volume fractions of silt, clay, and organic carbon. The strongest predictors for the sub-catchment stream were nitrogen and organic carbon content (although the former could not be included in the PLS of the main-stem). Jones et al. (1995) studied five streams (Strahler stream order 1) in central and southern Arizona and reported far greater methane production in hydrologically isolated river bank sediments, compared to parafluvial sediments interacting with the core flow. This reflects the connection with hydrology, geomorphology, and organic matter distribution in relation to CH_4 production in streams and is elaborated in the recent review of Stanley et al. (2016).

In the main-stem, porewater characteristics were generally less important drivers of PMP and PMO spatial variability than sediment indices. A positive relationship between Mn and methane production was also found by Qiao et al. (2015) in anaerobic batch experiments with wastewater. Mn may serve as an alternative electron donor for the process of methanogenesis from CO_2. The drivers of spatial variability for the sub-catchment stream, however, were more diverse than for the main-stem. We identified porewater DOM quality characteristics as highly influential drivers of PMP spatial variability (Figure 4b), which was, to our knowledge, observed for the first time. For example, the extent of humification, indicated by HIX, as well as aromaticity (SUVA254) were negatively correlated to PMP and PMO (Figure 4b), indicating that more degraded DOM produces less methane (Sobek et al., 2009).

Ultimately, the key drivers of PMP and PMO spatial variability in the main-stem were fine sediments, rich in organic matter (this study; Comer-Warner et al., 2018; Romeijn et al., 2019). These sediment properties are likely proxies for high microbial abundance, microbial diversity, and anoxia (Bushaw-Newton et al., 2012; Mendoza-Lera & Datry, 2017; Perkins et al., 2014). Moreover, fine sediments as a key driver for spatial variability of PMP and PMO is in accordance with Maeck et al. (2013) who found that sedimentation rate of fine sediment in river impoundments was the main control on their methane emissions. Small streams represent the largest water surface area of the global fluvial network (Downing et al., 2012), highlighting the importance of characterizing their emissions as part of the global methane budget. Our findings confirm, similar to reservoirs and impounded rivers, that sediment deposition and sediment composition are key controlling

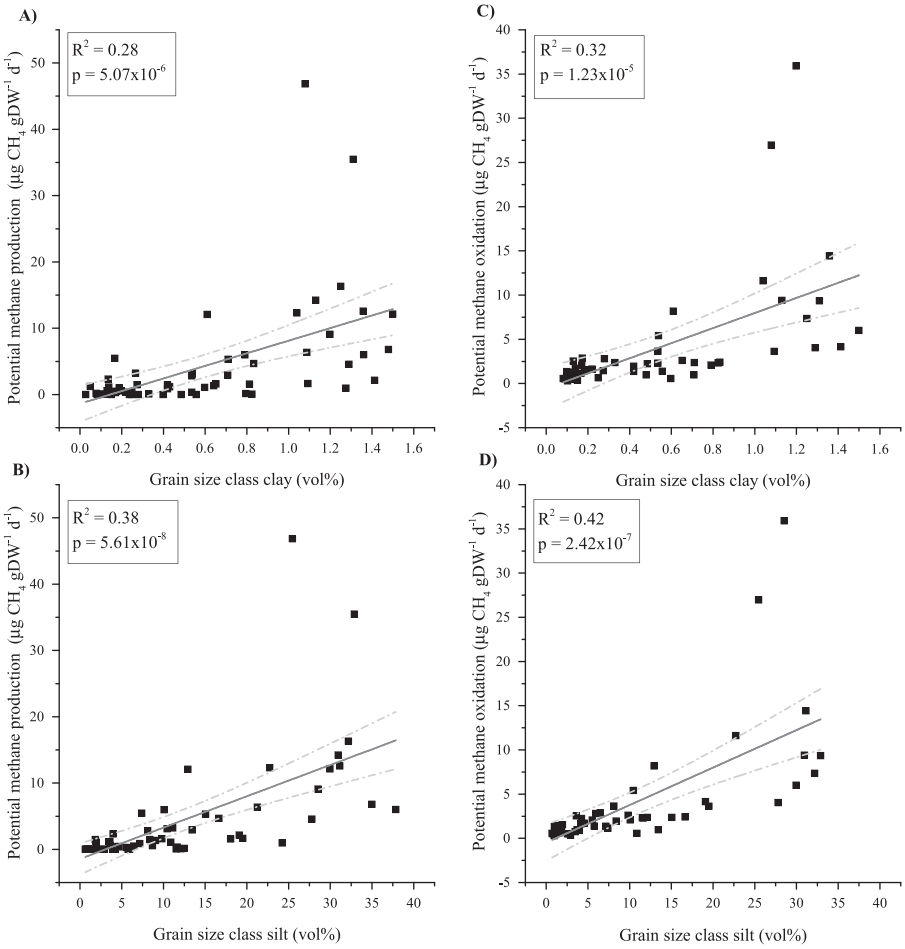

Figure 5. Linear regressions for potential methane production and grain size class clay (a) and silt (b) and for potential methane oxidation and grain size class clay (c) and silt (d). The solid line shows the linear regression, and the dash-dotted lines show the 95% confidence limits.

factors of their CH_4 emissions. The studies of Sanders et al. (2007) and Crawford and Stanley (2016) support this conclusion. Sanders et al. (2007) showed in the agricultural (76% of land use) River Frome in Dorset, England, a marked increase of silt/clay fraction in the sediment in spring and summer, this coincided with enhanced plant-mediated CH_4 emissions, and resulted in an increase in surface water CH_4 concentrations (and up to 100-fold increase in sediment CH_4 concentrations). Furthermore, Crawford and Stanley (2016) found strong evidence that increased sedimentation and enhanced organic matter content lead to higher methane emissions from streams draining human-impacted landscapes relative to pristine streams in northern Wisconsin (USA). Consequently, increasing deposition of fine sediments due to anthropogenic land disturbance, water abstraction, and flow regulation (Foley et al., 2005; Vörösmarty et al., 2000; Yuan et al., 2015) may have an amplifying effect on methane production in, and consequently methane emissions from, lotic systems (Comer-Warner et al., 2018). Conversely, extended droughts and irregular rainfall patterns could lead to increased drying-out of small streams in Europe due to the latitudinal amplification and periodic stalling of the gulf-stream (Francis & Vavrus, 2012, 2015; Martineau et al., 2017), thereby potentially off-setting increases.

Knowledge of the spatial distribution of preferential sediment deposition zones in stream networks can provide the basis for process-based models for methane emissions, such as those for wetlands and lakes (Sabrekov et al., 2017; Tang et al., 2010). Such models must be coupled with hydrological/hydraulic models, these may, in combination, facilitate regional to global scale CH_4 emission estimates, as already exist for CO_2 (Raymond et al., 2013). In headwater stream networks, the geomorphology gives rise to a patchy system over

scales of tens of meters (Noss & Lorke, 2016). The occurrence of elevated methane production patches will be dependent on hydraulic conditions that favor sediment settlement (Naden et al., 2016), and a supply of fine sediment, which is in-part related to the degree of catchment disturbance (Allan et al., 1997; Croke & Hairsine, 2006; Houser et al., 2006). In larger, higher-order rivers with lower slopes, an increase in the potential for fine sediment patches as a proportion of the river bed area is likely since overall hydraulic conditions favor a more general accumulation of fine sediment (Leitner et al., 2015; Wood & Armitage, 1997). The degree of catchment disturbance, for example, intensive agricultural land use with associated soil erosion and wash-off will control the supply of fine sediment (Naden et al., 2016) and hence the potential for enhanced methane production. Thus, hydraulically comparable river reaches with differing land use in their catchments may have very different CH_4 emission rates. Wilkinson, Bodmer, et al. (2019), for example, found impounded river reaches with minimal sediment and very low emissions. So although the presence of transverse structures, such as weirs, culverts, barrages, locks, and dams may provide conditions suited to hot-spot methane production (Maeck et al., 2013; Ollivier et al., 2019; Wilkinson, Bodmer, et al., 2019), sediment supply (i.e., lack of it) may limit this. Potentially, a mapping of hydraulic conditions, based-on slope, riverbed morphometry, and by inference stream power (sediment carrying capacity-siltation capacity) combined with land utilization intensity and a probabilistic estimate of methane production based-on observed data for different systems would be a significant step towards upscaling methane production from lotic systems.

To estimate CH_4 emissions at the landscape scale, it would be necessary to assess fine sediment spatial deposition patterns in flowing waters, based-on localized hydraulic conditions, as well as catchment sediment input. In addition, a broader range of data on the magnitude and drivers of PMP and PMO in smaller stream networks would help better constrain such estimates. Furthermore, a wider characterization of PMP and PMO across freshwater systems (e.g., lakes and reservoirs) would assist in the goal of upscaling emission estimates.

4.2. Relationship of PMP and PMO to Depth

Our study and others (e.g. Mach et al., 2015; Sanders et al., 2007) show that sediment depth is not a reliable predictor for PMP in small stream systems. The shallow water depth and predominantly energetic depositional environment, subject to rapid discharge variations, in our study catchment, is in sharp contrast to river impoundments, where consistent decline in PMP with depth was observed (e.g., Wilkinson et al., 2015; Wilkinson, Bodmer, et al., 2019). With the redistribution and mixing of materials, as well as re-inclusion of fresh and old organic matter, that gets buried quickly, for example, after storm events, it is not surprising that we found no consistent variations of PMP with sediment depth (Figure S5a). The most important drivers of PMP and PMO spatial variability in the main-stem and sub-catchment stream (sediment organic carbon and nitrogen content, and silt and clay) also had no consistent vertical gradients (Figures S6a–S6d). However, whether non-impounded streams with low flow velocity accompanied by strong deposition of fine sediments (e.g., heavily modified agricultural streams) behave more like larger river impoundments with a strong depth dependence of PMP (Maeck et al., 2013; Wilkinson et al., 2015; Wilkinson, Bodmer, et al., 2019) remains to be answered.

We found no consistent vertical gradients in PMO (Figure S5b). This is not surprising given the correlation with PMP and the influence of the fluvial environment as discussed above. Here we only measured PMO in the top 5 cm of the sediment, whereas Shelley et al. (2014), studying the River Lambourn in southern England, found methanotrophy (measured as PMO) to be active to at least 15 cm into the riverbed; the highest oxidation rates were in the upper 6 cm declining significantly with increasing depth. Buriánková et al. (2012) found a similar pattern, with greater methanotrophic activity in the top 25 cm compared to the deeper 25–50 cm of Sitka stream sediments (Czech Republic). Given a possible correlation of PMP and PMO, as seen here, those studies identifying strong PMP depth gradients may have had similar profiles for PMO.

4.3. Comparison of PMP and PMO With Literature Data and Explanatory Power of Our Data

Measuring protocols for PMP differ among studies presented in the literature, for example, incubation durations range from 24 hr (Crawford et al., 2017) to 4–6 weeks (this study; Bednařík et al., 2017), distilled water was added to incubation vials in some studies (Bednařík et al., 2017; Mach et al., 2015) and in others not (this study; Sanders et al., 2007; Wilkinson, Bodmer, et al., 2019). Despite these differences, our PMP rates were

within the range reported by Bednařík et al. (2017) for a second-order tributary of the Danube and Crawford et al. (2017) for a groundwater-dominated headwater stream. We measured the same order of magnitude as Sanders et al. (2007) for an agricultural river, but with a very high variability (indicated by standard deviations; Table S1) at the depths of 1 and 5 cm below the sediment-water interface (Figure S5a). We found far greater variability than Mach et al. (2015) who studied two cores from an agricultural stream, as opposed to the 26 cores studied here; they did not aim to sample a wide range of sediment; hence, the comparative difference in variability is not surprising.

There are several studies in streams where PMO was investigated (e.g., Bednařík et al., 2017; Sanders et al., 2007; Shelley et al., 2017). Shelley et al. (2015) demonstrated concentration dependent PMO at low CH_4 concentration; this highlighted the importance of initial CH_4 spiking concentration in incubations, and this concentration dependency also differed among sediment types. The corollary of this is that the potential for meaningful comparison of PMO estimates between studies is limited, and this shortcoming reveals an urgent need for standardized PMO measurement procedures.

We present data for idealized "potential" measurements of PMP and PMO, under in situ conditions, additional factors influence PMP and PMO. With hindsight, flow velocity measurements at each of our core sites would have been beneficial. Flow velocity controls sedimentation rate of fine material (e.g., Naden et al., 2016; e.g., clay and silt and associated organic carbon content), which was the key driver of PMP in our main-stem. Since low velocities favor settlement of fine sediment, a negative correlation between flow velocity, PMP, and PMO might have been observed. In addition, flow velocity affects oxygen penetration depth in sediment (Murniati et al., 2016) and consequently must influence the extent of PMO. This has relevance for the patterns of PMP and PMO that might be expected in flowing waters.

Higher flow velocities, compared to lower velocities, limit the settlement of fine material, increase the penetration depth of oxygen into the sediment, and accelerate gas exchange between the stream and the atmosphere (Raymond et al., 2012). These factors combine to influence porewater oxygen and CH_4 levels and, by inference, expected PMO rates. At low velocities, such as those found in river impoundments, conditions favor settlement of fine sediment, strongly anaerobic conditions, and high methane production, with bubbles bypassing the sediment matrix (Maeck et al., 2013), such that measured PMP and ebullitive flux may be in close agreement (e.g., Wilkinson et al., 2015), and PMO would be a small component of the methane budget. Conversely, in lakes, it has been found that up to 80% of the CH_4 produced can be oxidized (Bastviken et al., 2008), although this relates more to the relative supply of fine sediment than velocity. In a large fast flowing river such as the Amazon, ecosystem methane oxidation in the mainstream and its five largest tributaries has been reported to reduce CH_4 diffusive flux by 28–96% (Sawakuchi et al., 2016).

These varied findings indicate the importance of the supply of fine sediments and flow velocity with its relevance to settlement, gas transfer in the sediment, and gas exchange with the atmosphere. Hence, in flowing waters, where gas transfer and exchange are important, coupled PMO and PMP measurements are recommended to estimate CH_4 emission more accurately.

Acknowledgments
This study was financially supported by the German Research Foundation (DFG, Grant LO1150/5-2 and LO1150/9-1). We would like to thank Christoph Bors for assistance in the field and laboratory as well as Saskia Mertins, Sirma Scopchanova, and Dino Liesy for their support in the laboratory. Furthermore, we thank Felicity Shelley for her helpful suggestions regarding the potential methane oxidation method, Kurt Friese for enabling the grain size analyses and Michael Herzog for his support on site, as well as Markus Kurtz and Katrin Attermeyer for their support during data analysis. Finally, we would like to thank the reviewers for their constructive inputs which improved the manuscript. Data and metadata are available in the international research data repository Zenodo at [10.5281/zenodo.3565833].

References

Aben, R. C. H., Barros, N., van Donk, E., Frenken, T., Hilt, S., Kazanjian, G., et al. (2017). Cross continental increase in methane ebullition under climate change. *Nature Communications*, *8*(1), 1682. https://doi.org/10.1038/s41467-017-01535-y

Allan, D., Erickson, D., & Fay, J. (1997). The influence of catchment land use on stream integrity across multiple spatial scales. *Freshwater Biology*, *37*(1), 149–161. https://doi.org/10.1046/j.1365-2427.1997.d01-546.x

Bastviken, D. (2009). Methane. In G. E. Likens (Ed.), *Encyclopedia of inland waters*, (pp. 783–805). Oxford: Elsevier.

Bastviken, D., Cole, J. J., Pace, M. L., & Van de Bogert, M. C. (2008). Fates of methane from different lake habitats: Connecting whole-lake budgets and CH4 emissions. *Journal of Geophysical Research: Biogeosciences*, *113*(G2). https://doi.org/10.1029/2007jg000608

Bednařík, A., Blaser, M., Matoušů, A., Hekera, P., & Rulík, M. (2017). Effect of weir impoundments on methane dynamics in a river. *Science of the Total Environment*, *584-585*(Supplement C), 164–174. https://doi.org/10.1016/j.scitotenv.2017.01.163

Bernhardt, E. S., Blaszczak, J. R., Ficken, C. D., Fork, M. L., Kaiser, K. E., & Seybold, E. C. (2017). Control points in ecosystems: Moving beyond the hot spot hot moment concept. *Ecosystems*, *20*(4), 665–682.

Bodmer, P., Wilkinson, J., & Lorke, A. (2019). Sediment properties drive spatial variability of potential methane production and oxidation in small streams [1]. [Data set]. Retrieved from: https://doi.org/10.5281/zenodo.3565833

Bossard, P., Joller, T., & Szabó, E. (1981). Die quantitative Erfassung von Methan im Seewasser. *Schweizerische Zeitschrift für Hydrologie*, *43*(1), 200–211. https://doi.org/10.1007/bf02502482

Buriánková, I., Brablcová, L., Mach, V., Hýblová, A., Badurová, P., Cupalová, J., & Rulík, M. (2012). Methanogens and methanotrophs distribution in the hyporheic sediments of a small lowland stream. *Fundamental and Applied Limnology/Archiv für Hydrobiologie*, *181*(2), 87–102.

Bushaw-Newton, K. L., Ewers, E. C., Velinsky, D. J., Ashley, J. T., & MacAvoy, S. E. (2012). Bacterial community profiles from sediments of the Anacostia River using metabolic and molecular analyses. *Environmental Science and Pollution Research*, *19*(4), 1271–1279.

Cadieux, S. B., White, J. R., Sauer, P. E., Peng, Y., Goldman, A. E., & Pratt, L. M. (2016). Large fractionations of C and H isotopes related to methane oxidation in Arctic lakes. *Geochimica et Cosmochimica Acta*, *187*, 141–155.

Campeau, A., & Del Giorgio, P. A. (2014). Patterns in CH4 and CO2 concentrations across boreal rivers: Major drivers and implications for fluvial greenhouse emissions under climate change scenarios. *Global change biology*, *20*(4), 1075–1088. https://doi.org/10.1111/Gcb.12479

Ciais, P., Sabine, C., Bala, G., Bopp, L., Brovkin, V., Canadell, J., et al. (2013). Carbon and other biogeochemical cycles. In T. F. Stocker, D. Qin, G.-K. Plattner, M. Tignor, S. K. Allen, J. Boschung, A. Nauels, Y. Xia, V. Bex, & P. M. Midgley (Eds.), *Climate change 2013: The physical science basis. Contribution of working group I to the fifth assessment report of the Intergovernmental Panel on Climate Change* (chap. 6). Cambridge, United Kingdom and New York, NY, USA: Cambridge University Press.

Comer-Warner, S. A., Romeijn, P., Gooddy, D. C., Ullah, S., Kettridge, N., Marchant, B., et al. (2018). Thermal sensitivity of CO2 and CH4 emissions varies with streambed sediment properties. *Nature Communications*, *9*.

Crawford, J. T., Loken, L. C., West, W. E., Crary, B., Spawn, S. A., Gubbins, N., ... Stanley, E. H. (2017). Spatial heterogeneity of within-stream methane concentrations. *Journal of Geophysical Research: Biogeosciences, 122*(5), 1036-1048. doi: 10.1002/2016JG003698

Crawford, J. T., Lottig, N. R., Stanley, E. H., Walker, J. F., Hanson, P. C., Finlay, J. C., & Striegl, R. G. (2014). CO2 and CH4 emissions from streams in a lake-rich landscape: Patterns, controls, and regional significance. *Global Biogeochemical Cycles*, *28*(3), 197–210.

Crawford, J. T., & Stanley, E. H. (2016). Controls on methane concentrations and fluxes in streams draining human-dominated landscapes. *Ecological Applications*, *26*(5), 1581–1591. https://doi.org/10.1890/15-1330

Crawford, J. T., Striegl, R. G., Wickland, K. P., Dornblaser, M. M., & Stanley, E. H. (2013). Emissions of carbon dioxide and methane from a headwater stream network of interior Alaska. *Journal of Geophysical Research: Biogeosciences*, *118*(2), 482–494.

Croke, J. C., & Hairsine, P. B. (2006). Sediment delivery in managed forests: A review. *Environmental Reviews*, *14*(1), 59–87. https://doi.org/10.1139/a05-016

Cuthbert, I. D., & Del Giorgio, P. (1992). Toward a standard method of measuring color in freshwater. *Limnology and Oceanography*, *37*(6), 1319–1326.

Dahlen, J., Bertilsson, S., & Pettersson, C. (1996). Effects of UV-A irradiation on dissolved organic matter in humic surface waters. *Environment International, 22*(5), 501-506.

Dahm, V., Kupilas, B., Rolauffs, P., Hering, D., Haase, P., Kappes, H., ... Wagner, F. (2014). Strategien zur Optimierung von Fließgew€asser-Renaturierungsmaßnahmen und ihrer Erfolgskontrolle.

Dehaan, H. (1993). Solar UV-light penetration and photodegradation of humic substances in peaty lake water. *Limnology and Oceanography*, *38*(5), 1072–1076.

Downing, J. A., Cole, J. J., Duarte, C. A., Middelburg, J. J., Melack, J. M., Prairie, Y. T., et al. (2012). Global abundance and size distribution of streams and rivers. *Inland waters*, *2*(4), 229–236.

Eriksson, L., Johansson, E., Kettaneh-Wold, N., & Wold, S. (2001). *Multi-and megavariate data analysis: Principles and applications*. Umeå, Sweden: Umetrics AB.

Fellman, J. B., Hood, E., & Spencer, R. G. (2010). Fluorescence spectroscopy opens new windows into dissolved organic matter dynamics in freshwater ecosystems: A review. *Limnology and Oceanography*, *55*(6), 2452–2462. https://doi.org/10.4319/lo.2010.55.6.2452

Foley, J. A., DeFries, R., Asner, G. P., Barford, C., Bonan, G., Carpenter, S. R., et al. (2005). Global consequences of land use. *Science*, *309*(5734), 570–574. https://doi.org/10.1126/science.1111772

Francis, J. A., & Vavrus, S. J. (2012). Evidence linking Arctic amplification to extreme weather in mid-latitudes. *Geophysical Research Letters*, *39*(6).

Francis, J. A., & Vavrus, S. J. (2015). Evidence for a wavier jet stream in response to rapid Arctic warming. *Environmental Research Letters*, *10*(1), 014005.

Goldenfum, J. A. (2010). GHG measurement guidelines for freshwater reservoirs. In *Sutton, London: Derived From: The UNESCO/IHA greenhouse gas emissions from freshwater reservoirs research project*. (Chap. 3, p. 77). Sutton, London, United Kingdom: International Hydropower Association.

Hamdan, L. J., & Wickland, K. P. (2016). Methane emissions from oceans, coasts, and freshwater habitats: New perspectives and feedbacks on climate. *Limnology and Oceanography*, *61*(S1).

Harris, D., Horwáth, W. R., & van Kessel, C. (2001). Acid fumigation of soils to remove carbonates prior to total organic carbon or carbon-13 isotopic analysis. *Soil Science Society of America Journal*, *65*(6), 1853–1856.

Helms, J. R., Stubbins, A., Ritchie, J. D., Minor, E. C., Kieber, D. J., & Mopper, K. (2008). Absorption spectral slopes and slope ratios as indicators of molecular weight, source, and photobleaching of chromophoric dissolved organic matter. *Limnology and Oceanography*, *53*(3), 955–969. https://doi.org/10.4319/lo.2008.53.3.0955

Houser, J. N., Mulholland, P. J., & Maloney, K. O. (2006). Upland disturbance affects headwater stream nutrients and suspended sediments during baseflow and stormflow. *Journal of Environmental Quality*, *35*(1), 352–365.

Iacobucci, D., Schneider, M. J., Popovich, D. L., & Bakamitsos, G. A. (2016). Mean centering helps alleviate "micro" but not "macro" multicollinearity. *Behavior Research Methods*, *48*(4), 1308–1317. https://doi.org/10.3758/s13428-015-0624-x

Jaffé, R., McKnight, D., Maie, N., Cory, R., McDowell, W., & Campbell, J. (2008). Spatial and temporal variations in DOM composition in ecosystems: The importance of long-term monitoring of optical properties. *Journal of Geophysical Research: Biogeosciences (2005–2012)*, *113*(G4).

Jones, J. B., Holmes, R. M., Fisher, S. G., Grimm, N. B., & Greene, D. M. (1995). Methanogenesis in Arizona, USA dryland streams. *Biogeochemistry*, *31*(3), 155–173. https://doi.org/10.1007/bf00004047

Kling, G. W., Kipphut, G. W., & Miller, M. C. (1992). The flux of CO 2 and CH 4 from lakes and rivers in arctic Alaska. *Hydrobiologia*, *240*(1-3), 23–36.

Kothawala, D. N., Murphy, K. R., Stedmon, C. A., Weyhenmeyer, G. A., & Tranvik, L. J. (2013). Inner filter correction of dissolved organic matter fluorescence. *Limnology and Oceanography: Methods*, *11*(12), 616–630. https://doi.org/10.4319/lom.2013.11.616

Leitner, P., Hauer, C., Ofenböck, T., Pletterbauer, F., Schmidt-Kloiber, A., & Graf, W. (2015). Fine sediment deposition affects biodiversity and density of benthic macroinvertebrates: A case study in the freshwater pearl mussel river Waldaist (Upper Austria). *Limnologica*, *50*, 54–57. https://doi.org/10.1016/j.limno.2014.12.003

Mach, V., Blaser, M. B., Claus, P., Chaudhary, P. P., & Rulík, M. (2015). Methane production potentials, pathways, and communities of methanogens in vertical sediment profiles of river Sitka. *Frontiers in Microbiology*, *6*(506). https://doi.org/10.3389/fmicb.2015.00506

Maeck, A., DelSontro, T., McGinnis, D. F., Fischer, H., Flury, S., Schmidt, M., et al. (2013). Sediment trapping by dams creates methane emission hot spots. *Environmental science & technology*, *47*(15), 8130–8137. https://doi.org/10.1021/Es4003907

Martineau, P., Chen, G., & Burrows, D. A. (2017). Wave events: Climatology, trends, and relationship to Northern Hemisphere winter blocking and weather extremes. *Journal of Climate*, *30*(15), 5675–5697. https://doi.org/10.1175/jcli-d-16-0692.1

McGinnis, D. F., Bilsley, N., Schmidt, M., Fietzek, P., Bodmer, P., Premke, K., et al. (2016). Deconstructing methane emissions from a small Northern European river: Hydrodynamics and temperature as key drivers. *Environmental science & technology*, *50*(21), 11,680–11,687.

McKnight, D. M., Boyer, E. W., Westerhoff, P. K., Doran, P. T., Kulbe, T., & Andersen, D. T. (2001). Spectrofluorometric characterization of dissolved organic matter for indication of precursor organic material and aromaticity. *Limnology and Oceanography*, *46*(1), 38–48.

Mendoza-Lera, C., & Datry, T. (2017). Relating hydraulic conductivity and hyporheic zone biogeochemical processing to conserve and restore river ecosystem services. *Science of the Total Environment*, *579*, 1815–1821. https://doi.org/10.1016/j.scitotenv.2016.11.166

Murniati, E., Gross, D., Herlina, H., Hancke, K., Glud, R., & Lorke, A. (2016). Oxygen imaging at the sediment-water interface using lifetime-based laser induced fluorescence (τLIF) of nano-sized particles. *Limnology and Oceanography: Methods*.

Naden, P. S., Murphy, J. F., Old, G. H., Newman, J., Scarlett, P., Harman, M., et al. (2016). Understanding the controls on deposited fine sediment in the streams of agricultural catchments. *Science of the Total Environment*, *547*, 366–381. https://doi.org/10.1016/j.scitotenv.2015.12.079

Noss, C., & Lorke, A. (2016). Roughness, resistance, and dispersion: Relationships in small streams. *Water Resources Research*, *52*(4), 2802–2821. https://doi.org/10.1002/2015WR017449

Ohno, T. (2002). Fluorescence inner-filtering correction for determining the humification index of dissolved organic matter. *Environmental science & technology*, *36*(4), 742–746.

Ollivier, Q. R., Maher, D. T., Pitfield, C., & Macreadie, P. I. (2019). Punching above their weight: Large release of greenhouse gases from small agricultural dams. *Global change biology*, *25*(2), 721–732. https://doi.org/10.1111/gcb.14477

Oswald, K., Milucka, J., Brand, A., Littmann, S., Wehrli, B., Kuypers, M. M., & Schubert, C. J. (2015). Light-dependent aerobic methane oxidation reduces methane emissions from seasonally stratified lakes. *PloS one*, *10*(7), e0132574.

Palmer, M. A., Hakenkamp, C. C., & Nelson-Baker, K. (1997). Ecological heterogeneity in streams: Why variance matters. *Journal of the North American Benthological Society*, *16*(1), 189–202.

Parlanti, E., Worz, K., Geoffroy, L., & Lamotte, M. (2000). Dissolved organic matter fluorescence spectroscopy as a tool to estimate biological activity in a coastal zone submitted to anthropogenic inputs. *Organic Geochemistry*, *31*(12), 1765–1781. https://doi.org/10.1016/S0146-6380(00)00124-8

Perkins, T. L., Clements, K., Baas, J. H., Jago, C. F., Jones, D. L., Malham, S. K., & McDonald, J. E. (2014). Sediment composition influences spatial variation in the abundance of human pathogen indicator bacteria within an estuarine environment. *PloS one*, *9*(11), e112951.

Qiao, S., Tian, T., Qi, B., & Zhou, J. (2015). Methanogenesis from wastewater stimulated by addition of elemental manganese. *Scientific Reports*, *5*, 12732.

Raymond, P. A., Hartmann, J., Lauerwald, R., Sobek, S., McDonald, C., Hoover, M., et al. (2013). Global carbon dioxide emissions from inland waters. *Nature*, *503*(7476), 355–359.

Raymond, P. A., Zappa, C. J., Butman, D., Bott, T. L., Potter, J., Mulholland, P., et al. (2012). Scaling the gas transfer velocity and hydraulic geometry in streams and small rivers. *Limnology & Oceanography: Fluids & Environments*, *2*, 41–53.

Reeburgh, W. S., King, J. Y., Regli, S. K., Kling, G. W., Auerbach, N. A., & Walker, D. A. (1998). A CH4 emission estimate for the Kuparuk River basin, Alaska. *Journal of Geophysical Research: Atmospheres*, *103*(D22), 29,005–29,013. https://doi.org/10.1029/98jd00993

Romeijn, P., Comer-Warner, S. A., Ullah, S., Hannah, D. M., & Krause, S. (2019). Streambed organic matter controls on carbon dioxide and methane emissions from streams. *Environmental science & technology*, *53*(5), 2364–2374. https://doi.org/10.1021/acs.est.8b04243

Sabrekov, A. F., Runkle, B. R., Glagolev, M. V., Terentieva, I. E., Stepanenko, V. M., Kotsyurbenko, O. R., et al. (2017). Variability in methane emissions from West Siberia's shallow boreal lakes on a regional scale and its environmental controls. *Biogeosciences*, *14*(15), 3715.

Sanders, I., Heppell, C., Cotton, J., Wharton, G., Hildrew, A., Flowers, E., & Trimmer, M. (2007). Emission of methane from chalk streams has potential implications for agricultural practices. *Freshwater Biology*, *52*(6), 1176–1186.

Saunois, M., Bousquet, P., Poulter, B., Peregon, A., Ciais, P., Canadell, J. G., et al. (2016). The global methane budget 2000–2012. *Earth Syst. Sci. Data*, *8*(2), 697–751. https://doi.org/10.5194/essd-8-697-2016

Sawakuchi, H. O., Bastviken, D., Sawakuchi, A. O., Ward, N. D., Borges, C. D., Tsai, S. M., et al. (2016). Oxidative mitigation of aquatic methane emissions in large Amazonian rivers. *Global change biology*, *22*(3), 1075–1085. https://doi.org/10.1111/gcb.13169

Sekellick, A. J., Banks, W. S. L., & Myers, M. K. (2013). Water volume and sediment volume and density in Lake Linganore between Boyers Mill Road Bridge and Bens Branch, Frederick County, Maryland. In *2012 Scientific Investigations Report*, (p. 26). Reston, VA: U.S. Geological Survey.

Shelley, F., Abdullahi, F., Grey, J., & Trimmer, M. (2015). Microbial methane cycling in the bed of a chalk river: Oxidation has the potential to match methanogenesis enhanced by warming. *Freshwater Biology*, *60*(1), 150–160.

Shelley, F., Grey, J., & Trimmer, M. (2014). Widespread methanotrophic primary production in lowland chalk rivers. *Proceedings of the Royal Society of London B: Biological Sciences*, *281*(1783), 20132854.

Shelley, F., Ings, N., Hildrew, A. G., Trimmer, M., & Grey, J. (2017). Bringing methanotrophy in rivers out of the shadows. *Limnology and Oceanography*, *62*(6), 2345–2359. https://doi.org/10.1002/lno.10569

Shotbolt, L. (2010). Pore water sampling from lake and estuary sediments using Rhizon samplers. *Journal of Paleolimnology*, *44*(2), 695–700. https://doi.org/10.1007/s10933-008-9301-8

Sobek, S., Durisch-Kaiser, E., Zurbrügg, R., Wongfun, N., Wessels, M., Pasche, N., & Wehrli, B. (2009). Organic carbon burial efficiency in lake sediments controlled by oxygen exposure time and sediment source. *Limnology and Oceanography*, *54*(6), 2243–2254.

Sobek, S., Tranvik, L. J., Prairie, Y. T., Kortelainen, P., & Cole, J. J. (2007). Patterns and regulation of dissolved organic carbon: An analysis of 7,500 widely distributed lakes. *Limnology and Oceanography*, *52*(3), 1208–1219. https://doi.org/10.4319/lo.2007.52.3.1208

Stanley, E. H., Casson, N. J., Christel, S. T., Crawford, J. T., Loken, L. C., & Oliver, S. K. (2016). The ecology of methane in streams and rivers: Patterns, controls, and global significance. *Ecological monographs*, *86*(2), 146–171. https://doi.org/10.1890/15-1027

Tang, J., Zhuang, Q., Shannon, R., & White, J. (2010). Quantifying wetland methane emissions with process-based models of different complexities. *Biogeosciences*, *7*(11), 3817–3837.

Vörösmarty, C. J., Green, P., Salisbury, J., & Lammers, R. B. (2000). Global water resources: Vulnerability from climate change and population growth. *Science*, *289*(5477), 284–288.

Weishaar, J. L., Aiken, G. R., Bergamaschi, B. A., Fram, M. S., Fujii, R., & Mopper, K. (2003). Evaluation of specific ultraviolet absorbance as an indicator of the chemical composition and reactivity of dissolved organic carbon. *Environmental science & technology*, *37*(20), 4702–4708.

Wilkinson, J., Bodmer, P., & Lorke, A. (2019). Methane dynamics and thermal response in impoundments of the Rhine River, Germany. *Science of the Total Environment*, 1045–1057. https://doi.org/10.1016/j.scitotenv.2018.12.424

Wilkinson, J., Bors, C., Burgis, F., Lorke, A., & Bodmer, P. (2018). Measuring CO2 and CH4 with a portable gas analyzer: Closed-loop operation, optimization and assessment. *PloS one*, *13*(4), e0193973. https://doi.org/10.1371/journal.pone.0193973

Wilkinson, J., Bors, C., Burgis, F., Lorke, A., & Bodmer, P. (2019). Correction: Measuring CO2 and CH4 with a portable gas analyzer: Closed-loop operation, optimization and assessment. *PloS one*, *14*(3), e0206080. https://doi.org/10.1371/journal.pone.0206080

Wilkinson, J., Maeck, A., Alshboul, Z., & Lorke, A. (2015). Continuous seasonal river ebullition measurements linked to sediment methane formation. *Environmental science & technology*, *49*(22), 13,121–13,129.

Wood, P. J., & Armitage, P. D. (1997). Biological effects of fine sediment in the lotic environment. *Environmental management*, *21*(2), 203–217.

Yuan, J., Li, W., & Deng, Y. (2015). Amplified subtropical stationary waves in boreal summer and their implications for regional water extremes. *Environmental Research Letters*, *10*(10), 104009.

Yvon-Durocher, G., Allen, A. P., Bastviken, D., Conrad, R., Gudasz, C., St-Pierre, A., et al. (2014). Methane fluxes show consistent temperature dependence across microbial to ecosystem scales. *Nature*, *507*(7493), 488–491.

Reference From the Supporting Information

Sobek, S., Algesten, G., Bergström, A.-K., Jansson, M., & Tranvik, L. J. (2003). The catchment and climate regulation of pCO2 in boreal lakes. *Global change biology*, *9*(4), 630–641.